New Journal of Physics
The open access journal at the forefront of physics

Deutsche Physikalische Gesellschaft DPG
IOP Institute of Physics

Published in partnership with: Deutsche Physikalische Gesellschaft and the Institute of Physics

OPEN ACCESS

RECEIVED
18 February 2018

REVISED
4 June 2018

ACCEPTED FOR PUBLICATION
21 June 2018

PUBLISHED
4 July 2018

Original content from this work may be used under the terms of the Creative Commons Attribution 3.0 licence.

Any further distribution of this work must maintain attribution to the author(s) and the title of the work, journal citation and DOI.

PAPER

Making pions with laser light

W Schumaker[1,2], T Liang[1], R Clarke[3], J M Cole[4], G Grittani[5,6], S Kuschel[7], S P D Mangles[4], Z Najmudin[4], K Poder[4], G Sarri[8], D Symes[3], A G R Thomas[2], M Vargas[2], M Zepf[5,8] and K Krushelnick[2,9]

[1] SLAC National Accelerator Laboratory, Stanford University, Menlo Park, California 94025, United States of America
[2] Center for Ultrafast Optical Science, University of Michigan, Ann Arbor, Michigan 48109, United States of America
[3] Central Laser Facility, Rutherford Appleton Laboratory, Didcot, Oxfordshire OX11 0QX, United Kingdom
[4] The John Adams Institute for Accelerator Science, Blackett Laboratory, Imperial College London, London SW7 2BZ, United Kingdom
[5] Institute of Physics ASCR, v.v.i. (FZU), ELI Beamlines project, Na Slovance 2, 18221 Prague, Czechia
[6] Czech Technical University in Prague, FNSPE, Brehova 7, 11519 Prague, Czechia
[7] Helmholtz Institute Jena, Frobelstieg 3, D-07743 Jena, Germany
[8] School of Mathematics and Physics, The Queen's University of Belfast, Belfast, BT7 1NN, United Kingdom
[9] Author to whom any correspondence should be addressed.

E-mail: kmkr@umich.edu

Keywords: lasers, accelerators, plasmas, particle sources

Abstract

The interaction of high intensity short pulse laser beams with plasmas can accelerate electrons to energies in excess of a GeV. These electron beams can subsequently be used to generate short-lived particles such as positrons, muons, and pions. In recent experiments, we have made the first measurements of pion production using 'all optical' methods. In particular, we have demonstrated that the interaction of bremsstrahlung generated by laser driven electron beams with aluminum atoms can produce the long lived isotope of magnesium (^{27}Mg) which is a signature for pion (π^+) production and subsequent muon decay. Using a 300 TW laser pulse, we have measured the generation of 150 ± 50 pions per shot. We also show that the energetic electron beam is a source of an intense, highly directional neutron beam resulting from (γ, n) reactions which contributes to the ^{27}Mg measurement as background via the (n, p) process.

Over the past several years, there have been many experiments which have demonstrated that high-energy quasi-monoenergetic electron beams can be produced as a result of the interaction of intense short pulse lasers with underdense plasmas (laser wakefield acceleration). Relativistic electrons can be produced through acceleration [1] by large amplitude relativistic plasma waves in the 'bubble' regime which are created in the wake of the laser pulse as it propagates through low density plasma [2–4]. Recently, electrons with greater than 1 GeV energy have been generated using short laser pulses as they propagate through extended plasmas [5–7]. These high-energy electrons can consequently produce gamma rays [8–10] through interaction with matter and such gamma rays can subsequently be used as sources of positrons [11–13], neutrons [14], and potentially more 'exotic' particles such as pions and muons [15–18]. We have recently used such energetic electron beams to generate highly directional positron sources with energies greater than 100 MeV [13] as well as energetic directional neutron beams [14].

Although positrons are anti-matter, they are produced naturally via β^+ decay. Similarly, neutrons—which are naturally bound to the nucleus—can be ejected via nuclear fusion, spontaneous fission, etc. As such, both neutrons and positrons can be produced with terrestrial, non-accelerator sources. However, more exotic particles requiring higher rest mass (>100 MeV/c^2) than typically available from natural radioactive processes (decay, fusion, fission) must be created using high-energy particles either from a cosmic source or an accelerator [19–21]. Moreover, unlike the relatively stable half-lives of positrons (>10^{46} s) and neutrons (881 s), all of these higher-energy particles have half-lives of 2 μs or less, making synchronization crucial for potential applications and controlled measurements.

Pions are the lightest meson (a particle consisting of a quark and an anti-quark) having a rest mass of 140 MeV/c^2 and are a key decay product in high-energy particle physics experiments. Despite having a larger

© 2018 The Author(s). Published by IOP Publishing Ltd on behalf of Deutsche Physikalische Gesellschaft

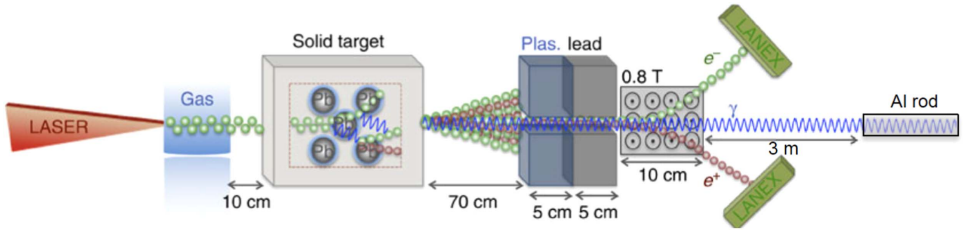

Figure 1. Simplified experimental geometry for measuring pion/neutron production.

rest mass than a muon, they require less energy to produce with gamma rays since a (virtual) quark/anti-quark pair (>140 MeV) in a nucleus is easier to produce than a muon/anti-muon pair (>212 MeV). However, these quark/anti-quark pairs must be created with enough energy to overcome the binding energy of the quarks in the neutron or proton with which it is interacting so that it can transfer quarks and form a pion. This process also leads to neutron/proton transformation inside the nucleus and can form a different element/isotope than the original nucleus.

In certain cases, the new element is a radioactive isotope, which can be readily measured and identified *ex situ* with a high-purity germanium (HPGe) detector. This is quite useful for the detection of pions since they are difficult to measure directly and have an extremely short life time (26 ns) before preferentially (>99.988%) decaying into longer-lived (and nearly as difficult to directly detect) muons. However, due to the inherently low production cross-sections (10–100 μb) for pions, care must be taken to account for other primary and secondary processes such as (γ, n) and (n, p), which can result in the same isotope as (γ, π^+) processes. Increasing the length of interaction can cause a significant production of the identifying isotope from secondary processes as the primary process yield increases. To minimize these secondary processes, previous experiments on pion production at synchrotron sources used a thin (100 μm) activation target. However, due to the much lower average flux on current laser wakefield accelerators (LWFA) compared to conventional accelerators, one must sacrifice accuracy for yield to obtain significant activation. In this case, the ^{27}Al$(\gamma, \pi^+)^{27}$Mg interaction is ideal for measuring pion production since it has a half-life of 9.46 min and is a β-emitter with clear γ-ray signatures having lines at 843.7 keV (71.8% branching ratio) and 1014.55 keV (28.2% branching ratio), which are easily measurable with a HPGe detector.

In this paper, we discuss experiments using the high power Astra-Gemini laser at the Rutherford Appleton Laboratory which were conducted to demonstrate for the first time that pions can be generated through all optical means on a 'table-top' laboratory experimental set-up. We set out to detect π^+ via the ^{27}Al$(\gamma, \pi^+)^{27}$Mg reaction which has a threshold of 140 MeV (see cross-section in [21]). In this case, the pion detector consisted simply of aluminum posts which were placed co-axially with the photon beam (figure 1). The aluminum rods were built into a plastic block to moderate and attenuate external (γ, n) neutrons from the surrounding shielding and were straddled by energy-sensitive (10 keV–20 MeV) neutron bubble detectors. The aluminum rods had a diameter of 1.25 cm and a total length of 20 cm, consisting of 4 $\times$ 5 cm rods so as to fit within the HPGe detector housing used to measure the induced activation. At both ends of the plastic block, an x-ray sensitive image plate was mounted to the block to determine the alignment of the rods with respect to the incident photon beam. After a sequence of shots, the rods were analyzed in the HPGe detector (see figure 2). However to account for the effects of neutron generated background for this isotope, the neutrons were also measured simultaneously in the experiment. The experimental results were then compared with FLUKA Monte-Carlo simulations of the experiment. In the HPGe spectra, 25 counts of the 843 keV line were measured indicating 180 ^{27}Mg/shot and 6 counts of the 1014 keV line were measured indicating 110 ^{27}Mg/shot.

Note that there were also additional peaks due to trace reactions observed in the irradiated sample. In particular, the (n, p) reaction with ^{56}Fe produces ^{56}Mn which is radioactive with a 2.58 h half-life (843 keV). Also in the sample there was a trace amount of ^{40}K which is radioactive generating a line at 1460 keV.

For this experiment, the electron beam was generated and accelerated during the propagation of the intense Astra-Gemini laser beam through a 2 cm long gas-cell filled with He at a background pressure of 60 mbar. Once fully ionized, this corresponds to an electron density of 3 $\times$ 10^{17} cm^{-3}, as extracted from optical interferometry of the plasma. The laser (pulse duration of 42 $\pm$ 3 fs) was focussed using an f/40 spherical mirror. The interaction accelerated electrons with a broad spectra up to 1 GeV containing a total charge of 300 pC. The electron beam overall charge and spectral shape are stable within 10% (as observed over 10 consecutive shots). The electron beam divergence is measured, by looking at the electron beam diameter 2 m downstream of the gas-cell, to be energy-dependent and of the order of ~5 mrad for electron energies exceeding a few hundred

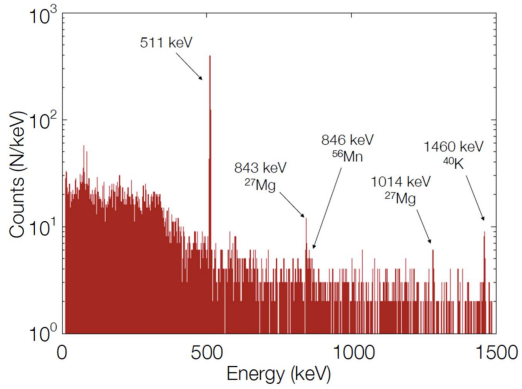

Figure 2. Emission spectrum from Al sample integrated over 30 min after 16 electron beam shots.

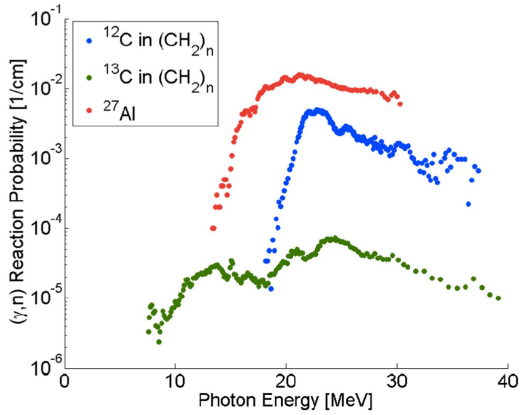

Figure 3. Cross-sections for (γ, n) processes from EXFOR.

MeV. Assuming full loading of the laser wakefield bubble, the electron beam duration can be estimated to be of the order of 60 fs. Space charge effects appear to be negligible for electron energies exceeding 100 MeV, justifying the assumption of the electron beam divergence being constant throughout the propagation to the detector.

The beam was passed through a 1.5 cm thick Pb converter before the electrons/positrons were separated by a spectrometer magnet. The radiation length of Pb is ~0.3 cm so the bremsstrahlung spectrum (as simulated by a Monte-Carlo code) has a similar number of photons as the number of electrons in the beam and an endpoint of ~1 GeV [22]. After 4.2 m, the transmitted photons interacted with the 20 cm long Al rod surrounded by a high-density polyethylene (HDPE) holder. Neutrons were detected by 3 sets of 6 energy-sensitive bubble detectors with separate energy thresholds of 0.01, 0.1, 0.6, 1.0, 2.5, and 10.0 MeV. These were placed adjacent to the Al rod within the HDPE holder. We estimate that the highest energy portion of the gamma-ray beam had diverged to about 2 cm in diameter after 4.2 m of propagation so that the probability of the beam also interacting with the HDPE holder must be considered. The relative reaction probabilities between the Al and HDPE are shown in figure 3 [23], which indicates that the carbon in the HDPE can make neutrons at higher photon energies. However, because the (γ, n) energy threshold of aluminum is much lower and its cross-section is relatively higher, neutrons from carbon will not contribute as much to the high-energy bins, rather adding signal to the lower energy bins. Assuming the neutrons are predominantly generated in the aluminum due to its significantly higher cross-section, the measured neutrons imply that the incident photon energy is at least 15 MeV greater than the resultant neutron energy due to the requirement to overcome the binding energy of the aluminum nucleus.

After a shot series, the bubble detectors were removed and counted for the number of bubbles or expansions in the superheated emulsion caused by a capture of a neutron. The neutron spectra can be determined by de-convolving bubbles from detectors with different energy thresholds. However, for this case, we are primarily interested in only the high-energy portion of the spectra (>1 MeV) since the highest energy bins are more clearly resolved (the highest-energy signal is directly proportional to its neutron flux). There were three different conditions tested. First, as a background shot, we did not use a converter target (no bremsstrahlung) and

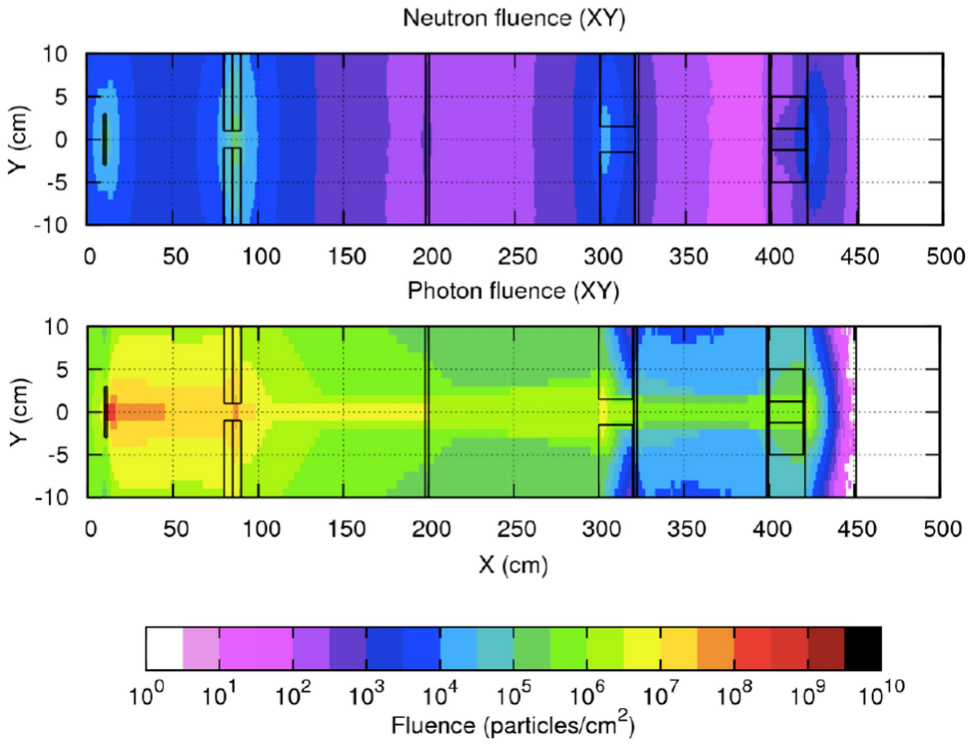

Figure 4. Monte-Carlo simulation results showing neutron (top) and high-energy photon (bottom) fluences in the experimental geometry.

deflected the electrons with a magnet. Next, we installed a 1.5 cm thick Pb converter to generate bremsstrahlung photons but magnetically deflected the e^-/e^+. Finally, we removed both the converter and magnet to allow the electrons to propagate to the target and create bremsstrahlung closer to (or inside of) the detector. The average neutron fluence for each one of these cases was obtained after spectral de-convolution.

For the case with only bremsstrahlung photons entering the detectors, we measured 5×10^6 neutrons/shot above 2.5 MeV and 5×10^5 neutrons/shot above 10 MeV. Since only the high-energy low divergence part of the beam was measured, the total flux of neutrons from such experiments is expected to be much higher. Due to conservation of momentum, the (γ, n) neutrons will receive a kick along the direction of the incident photon. This anisotropy results in an effective beamed source of neutrons.

After a series of 10–20 shots, the bubble detectors in the array were removed and counted. For the neutrons less than 10 MeV, the ratio was approximately 4.75 inner/outer ratio, implying the beam was directional in a forward cone of roughly 80°. For neutrons greater than 10 MeV, the signal is entirely contained in the inner ring of detectors, placing the upper limit of the divergence at 32° based on the geometry. For one series in particular, this was evident as 1.7 bubbles/shot (corresponding to 4.1×10^6 neutrons/shot with roughly 200 cm^2 detector area) between 10–20 MeV were counted in the inner ring, while none were seen on the outer track over 10 shots.

We also performed Monte-Carlo simulations of these experiments (see figure 4). Given the bremsstrahlung photon spectrum from a 1 GeV, 300 pC flat-spectra electron beam interacting with 1.5 cm of Pb, the number of ^{27}Al(γ, n)^{26}Al activations would be 5×10^7 neutrons/shot. However, this assumes primary interactions only with flat cross-sections, neglecting any cascading effects which may be significant since the cross-section is peaked at lower photon energies as we saw only 25 counts from 843 keV (the primary decay gamma of ^{27}Mg) and more than 80% of this is expected from (γ, π^+) rather than (n, p) based on the 0.8 GeV photon spectrum. Using a more realistic photon spectrum of >800 MeV would skew this ratio even more in favor of (γ, π^+). Given the low level of ^{27}Mg, accurately determining the level of pion production compared to (n, p) could only be done using a detailed Monte-Carlo treatment with the full detector/shielding geometry as done here.

Assuming each shot created the same number of activations, the FLUKA Monte-Carlo code can be used to estimate the number of pions created per shot. The measured activity is back-extrapolated from knowing the amount of time that the sample decayed after the final shot (13 min) and the number of shots taken over a given time (16 shots at 1 shot every 40 s). Therefore, measuring 25 counts on the 10% inherently efficient HPGe detector collecting ~50% of the total solid angle infers that 180 ^{27}Mg activations/shot were generated (see table 1). Since 80% of these ^{27}Mg activations are estimated (from FLUKA simulations) to come from (γ, π^+), the

Table 1. Summary of results.

Quantity	843 keV	1014 keV
Raw counts	25	6
Branching ratio	71.8%	28.2%
Detector efficiency	10%	10%
Solid angle collection	50%	50%
Measured ^{27}Mg /shot	180	110
Simulated ^{27}Mg /shot	106	

estimated pion number was found to be 150 pions/shot. The uncertainty is estimated to be ±50 as a result of background and standard error statistics.

Since the charged pions preferentially decay into a muon of the same charge for 99.988% of decays, the detection of charged pions is also an effective indirect measurement of muons. Therefore, for nearly every measured pion, there is a muon produced. From the pion measurements in the previous section, the number of muons per shot at Astra-Gemini could be inferred to be ~150 muons/shot.

In conclusion, secondary particle generation data has been presented using LWFA electrons as the driver yielding the first directional neutron beam measurement using LWFA, and the first measured production of pions (and inferred muons) using lasers. These results demonstrate the unique capabilities of laser wakefield acceleration sources of particles and radiation and show that new and potentially important applications are now becoming possible.

There are many new even higher power laser facilities under construction (up to 10 Petawatts) which will be capable of generating much higher fluxes of both pions and muons [24–26]. Such sources can be used for calibrating detectors, as injection sources for muon accelerators as well as for applications such as muon radiography.

Acknowledgments

We are grateful for the support of the Central Laser Facility staff. The work of WS and TL was supported by DOE FES through FWP 100182. The work of WS, AGRT, and KK was partially supported by funding from the National Science Foundation CAREER award (1054164), DOE (Grant No. DE-NA0002372) and ARO (Grant No. W911NF-16-1-0044). GS and MZ acknowledge funding from the Engineering and Physical Sciences Research Council grants (EP/L013975/1 and EP/I029206/1). GG was supported by the Consiglio Nazionale delle Ricerche (ELI-Italy) and Insitutio Nazionale di Fisica Nucleare (CN5-g-RESIST). SPDM, JMC and KP acknowledge financial support from STFC grant (ST/J002062/1).

ORCID iDs

S P D Mangles https://orcid.org/0000-0003-2443-4201
Z Najmudin https://orcid.org/0000-0001-6323-4005
K Poder https://orcid.org/0000-0002-0329-3510
K Krushelnick https://orcid.org/0000-0001-9116-9511

References

[1] Tajima T and Dawson J M 1979 *Phys. Rev. Lett.* **43** 267
[2] Faure J, Glinec Y, Pukhov A, Kiselev S, Gordienko S, Lefebvre E, Rousseau J-P, Burgy F and Malka V 2004 *Nature* **431** 541
[3] Mangles S P D *et al* 2004 *Nature* **431** 535
[4] Geddes C G R, Toth C, van Tilborg J, Esarey E, Schroeder C B, Bruhwiler D, Nieter C, Cary J and Leemans W P 2004 *Nature* **431** 538
[5] Leemans W P, Nagler B, Gonsalves A J, Toth C, Nakamura K, Geddes C G R, Esarey E, Schroeder C B and Hooker S M 2006 *Nat. Phys.* **2** 696
[6] Wang X *et al* 2013 *Nat. Commun.* **4** 1988
[7] Kneip S *et al* 2009 *Phys. Rev. Lett.* **103** 035002
[8] Edwards R D *et al* 2002 *Appl. Phys. Lett.* **80** 2129
[9] Reed S A *et al* 2006 *Appl. Phys. Lett.* **89** 231107
[10] Ledingham K W D *et al* 2000 *Phys. Rev. Lett.* **84** 899
[11] Gahn C, Tsakiris G D, Pretzler G, Witte K J, Delfin C, Wahlstrom C-G and Habs D 2000 *Appl. Phys. Lett.* **77** 2662
[12] Chen H *et al* 2010 *Phys. Rev. Lett.* **105** 015003
[13] Sarri G *et al* 2013 *Phys. Rev. Lett.* **110** 255002
[14] Zulick C *et al* 2013 *Appl. Phys. Lett.* **102** 124101

[15] Karsch S, Habs D, Schatz T, Schramm U and Pukhov A 1999 *Laser Part. Beams* **17** 565
[16] Ledingham K and Galster W 2010 *New J. Phys.* **12** 045005
[17] Bychenkov V Y, Sentoku Y, Bulanov S V, Mima K, Mourou G and Tolokonnikov S V 2001 *J. Exp. Theor. Phys. Lett.* **74** 586
[18] Di Piazza A, Muller C, Hatsagortsyan K and Keitel C 2012 *Rev. Mod. Phys.* **84** 1177
[19] Devanathan V, Prasad G N S and Rao K S 1973 *Phys. Rev.* C **8** 188
[20] Andersson G, Blomqvist I, Forkman B, Johnsson G G, Jarund A, Kroon I, Lindgren K, Schroder B and Tesch K 1972 *Nucl. Phys.* A **197** 44
[21] Kuz'menko V, Mitrofanova A V, Noga V I, Ranyuk Y N, Sorokin P V, Telegin Y N, Blomqvist I, Jonsson G G and Freed N 1977 *Phys. Rev.* C **16** 1513
[22] Schumaker W *et al* 2014 *Phys. Plasmas* **21** 056704
[23] McLane V, Kellett M, Schwerer O and Maev S 2002 *J. Nucl. Sci. Technol.* **39 Suppl. 2** 1458
[24] Zamfir N V 2014 *Eur. Phys. J. Spec. Top.* **223** 1221
[25] Mourou G and Tajima T 2014 *Eur. Phys. J. Spec. Top.* **223** 979
[26] Tommasini D, Ferrando A, Michinel H and Seco M 2009 *J. High Energy Phys.* JHEP11(2009)043